Control of the inverse pendulum based on sliding mode and model predictive control

Schwab, Karl Christian; Schräder, Lennart; Mercorelli, Paolo; Lassen, Jan Thore

Published in:
WSEAS Transactions on Systems and Control

Publication date:
2018

Document Version
Publisher's PDF, also known as Version of record

Control of the Inverse Pendulum Based on Sliding Mode and Model Predictive Control

KARL-CHRISTIAN SCHWAB[1], LENNART SCHRÄDER[1], PAOLO MERCORELLI[1], JAN THORE LASSEN[1]
[1] Institute for Product and Process Innovation
Leuphana University of Lueneburg
Universitätsallee 1, 21335 Lueneburg
GERMANY
mercorelli@uni.leuphana.de
https://www2.leuphana.de/mercorelli

Abstract: In the present work two different rules are applied to the system of the inverse pendulum. On the one hand, Sliding Mode Control (SMC) is used to control the position and the angular velocity of the pendulum attached to the cart. On the other hand, Model Predictive Control (MPC) is implemented in order to control the trajectory of the cart in accordance with a desired movement profile. In order to counteract phenomena such as "chattering" as effectively as possible, various measures are implemented within the Sliding Mode Control.

Key-Words: Inverted pendulum, Model Predictive Control, Sliding Mode Control, underactuated system

1 Introduction

The inverse pendulum represents an underactuated system in which the unstable rest position is located at the highest point of the pendulum. In order to regulate this system, that means to keep the angle between the pendulum and the vertical axis minimal or equal to zero, the cart can be moved in one axis with the help of an applied force. Since the system is underactuated, it has fewer actuators than degrees of freedom. This type of system is common, including for robots [1] [2].

Sliding Mode Control, a system based on the Lyapunov theorem, provides the ability to regulate underactuated systems effectively. In general, SMC is a very accurate and robust control system which effectively counteracts disturbances both internal and external [3]. Due to the computation by means of the equations of motion and the associated restrictions, the Sliding Mode Control regulates not only the angle but also the angular velocity of the pendulum. This limitation arises because the force exerted does not act directly on the pendulum, but instead on the cart, whose movement affects the rotation and the angular speed of the pendulum. Both control variables are to be regulated to zero, so that the pendulum is in the equilibrium position and is moving as slowly as possible.

As a second control system Model Predictive Control is introduced to control the trajectory of the cart in accordance with a desired movement profile. MPC predicts future values for both the state variables and the output variables of the system based on measurements and a discrete-time dynamic model of the process. On this basis, it is possible to calculate future results for k time steps in advance [4]. The prediction of future behaviour allows the calculation of an optimal input signal to replicate the desired trajectory as much as possible. For the application of this type of Model Predictive Control a linearization of the system is required. The linearization is based on the small angle approximation as well as on the linearization at an operating point. The selected operating point in this case corresponds to the equilibrium position of the inverse pendulum.

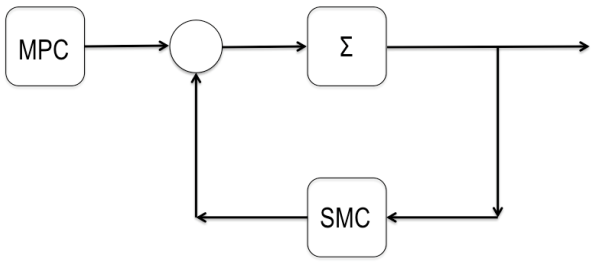

Fig. 1: Block diagram control loop

The system is simulated using Simulink and Matlab. To test the functionality and the robustness of the arrangements, an initial angle is applied on the one hand and, on the other hand, noise is introduced into the system. Basically, the use of two control systems with different control variables, which are linked to each other, creates a conflict. The impact of this conflict will be analysed at the end of this work.

Both, the characteristics of the system and the mechanisms that will be used for controlling the inverse pendulum, can be found in different everyday life systems. For example, Segways have similar characteristics as the inverse pendulum. Therefore, similar rules can be used for controlling the Segway. Also, for the control of rockets during launch and landing as well as for the balancing of robots' similar principles are used [5].
In the following sections, the system of the inverse pendulum is described (Chapter 2). Subsequently, steps for implementing the SMC (Chapter 3) and the MPC (Chapter 4) are explained. Finally, the behaviour of the controlled system is analysed (Chapter 5).

2 Description of the System of the Inverse Pendulum

The dynamic behaviour of the inverse pendulum can be described by the following equations of motion [6]:

$$J\ddot{\alpha}(t) = -F_g l\, sin\alpha(t) + m_p \ddot{x}(t) l\, cos\alpha(t) - k_w \dot{\alpha}(t), \quad (1)$$

$$\left(m_p + m_{Fgz}\right)\ddot{x}(t) = F_c sin\alpha(t) - F_T cos\alpha(t) - k_l \dot{x}(t) + F \quad (2)$$

J corresponds to the moment of inertia of the pendulum, F_g is the weight force, l is the length of the pendulum, m_p and m_{fzg} are the mass of the pendulum and the vehicle, k_w is a combination of air and rolling friction of the vehicle and k_l is the friction in the point of contact between the vehicle and pendulum, F_T the tangential force and F_c is the centrifugal force resulting from the rotational movement. The input parameter corresponds to the force F, which is applied directly to the cart.

Table 1: Definition of equation symbols

Meaning	Equation
Tangential force F_T	$F_T = m_p l \ddot{\alpha}(t)$
Centrifugal force F_C	$F_C = m_p l\, \dot{\alpha}(t)^2$
Horizontal force F_{or}	$F_{or} = m_p \ddot{x}(t)$
weight force F_g	$F_g = m_p\, g$
moment of inertia J	$J = m_p\, l^2$
torque M	$M = J\ddot{\alpha}(t) = m_p\, l^2\, \ddot{\alpha}(t)$

For simplicity, it has been assumed that the rod of the pendulum has no mass. The system is represented in figure 2.

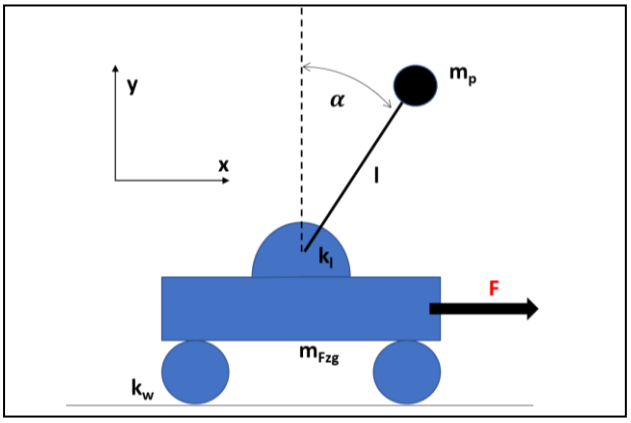

Fig.2: Representation of the system

3 Implementation of Sliding Mode Control

Sliding Mode Control is a very robust and accurate control system. Based on the Lyapunov theorem, the system can be controlled in the position of equilibrium, without knowing the solution of the underlying system of equations. For the implementation of the Sliding Mode Control a so-called cost function s(t) must be set up, which is a target-actual comparison between the real and the desired output variables [3]. In the present case the angle between the pendulum and the vertical axis as well as the angular velocity of the pendulum are the control variables.

$$s(t) = k * \left(\alpha_d(t) - \alpha(t)\right) + \dot{\alpha}_d(t) - \dot{\alpha}(t)\ . \quad (3)$$

The variable k was introduced as a factor for the weighting of the error between the desired and the actual angle. Since both, the desired angle $\alpha_d(t)$ and the desired angular velocity $\dot{\alpha}_d(t)$, are zero, the cost function results to:

$$s(t) = k * \left(-\alpha(t)\right) - \dot{\alpha}(t). \quad (4)$$

For the implementation of the Sliding Mode Control the equations need to be drawn up according to the following Lyapunov model:

$$1a.\ V(s(t)) > 0, \quad (5)$$

$$1b.\ V(0) = 0, \quad (6)$$

$$2.\ \dot{V}(s(t)) < 0. \quad (7)$$

By choosing the function (8) for $V(s(t))$, condition 1a is fulfilled.

$$V(s(t)) = \frac{1}{2}s^2(t) \tag{8}$$

Accordingly, $\dot{V}(s(t))$ results to:

$$\dot{V}(s(t)) = s(t) * \dot{s}(t) = s(t) * [-k * \dot{\alpha}(t) - \ddot{\alpha}(t)] \ , \tag{9}$$

$$\dot{V}(s(t)) = s(t) * \left[-k * \dot{\alpha}(t) - \frac{m_p * g * l * sin\alpha(t)}{J} - \frac{{m_p}^2 * l^2 * cos\alpha(t) * \dot{\alpha}^2(t) * sin\alpha(t)}{J * (m_{Fzg} + m_p)} + \frac{{m_p}^2 * l^2 * cos^2\alpha(t) * \ddot{\alpha}(t)}{J * (m_{Fzg} + m_p)} + \frac{k_l * \dot{x}(t) * m_p * l * cos\alpha(t)}{J} - \frac{k_w * \dot{\alpha}(t)}{J} + \frac{F(t)}{J * (m_{Fzg} + m_p)} + \frac{d(t)}{J}\right]. \tag{10}$$

In the subsequent step, the input F(t) is established so that the system can be controlled by cancelling most of the variables of the system. The resulting force is structured as follows:

$$F(t) = -k * \dot{\alpha}(t) * J * (m_{Fgz} + m_p) - m_p * g * l * sin\alpha(t) * (m_{Fgz} + m_p) + {m_p}^2 * l^2 * cos\alpha(t) * \dot{\alpha}^2(t) * sin\alpha(t) + {m_p}^2 * l^2 * cos^2\alpha(t) * \ddot{\alpha}(t) - k_l * \dot{x}(t) * m_p * l * cos\alpha(t) * (m_{Fgz} + m_p) - k_w * \dot{\alpha}(t) * (m_{Fgz} + m_p) - (\beta * sign(k * -\alpha - \dot{\alpha}) \ . \tag{11}$$

As a result of the implementation of F(t) we gain for $\dot{V}(s(t))$:

$$\dot{V}(s(t)) = s(t) * \left[-\beta * sign(s(t)) * \frac{l * cos\alpha(t) * m_p}{J * (m_{Fzg} + m_p)} + \frac{d(t)}{J}\right] . \tag{12}$$

To satisfy the statement in condition (7), β needs to be:

$$\beta > (m_{Fzg} + m_p) * \frac{\max(d(t))}{l * \cos(\alpha) * m_p} . \tag{13}$$

When implementing those functions in Matlab, it can be seen that the force switches back and forth very quickly between -100 N and 100 N. This phenomenon, which is called chattering, results from the use of the sign function. A corresponding fast switching of the input variables is often impossible or undesirable. To prevent this high-frequency "switching", a saturation function is used instead of the sign function. This prevents fast switching, because a linear function instead of a discontinuous function (sign function) is used within the defined range Φ. However, it should be noted that after using the saturation function, the accuracy of the control decreases [3].

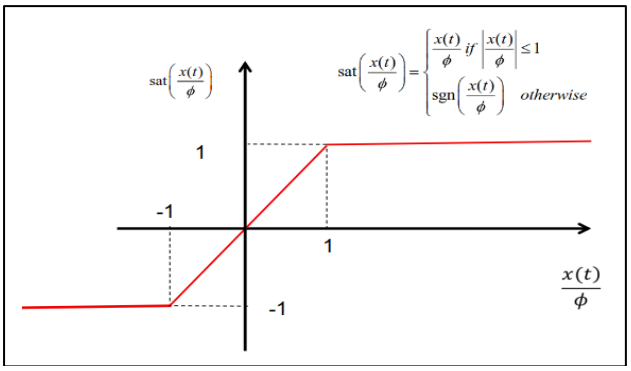

Fig. 3: Saturation function

By using the saturation function, the following force F(t) results:

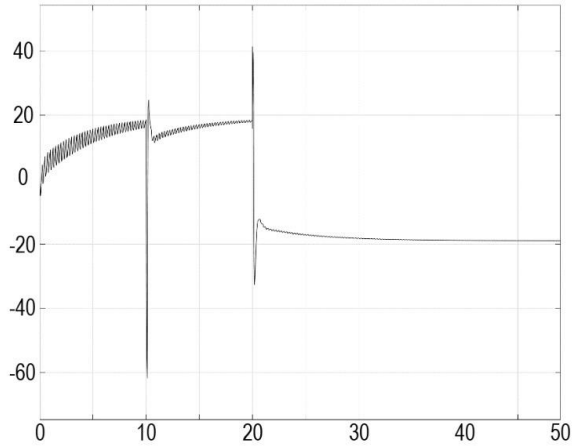

Fig. 4: Force F(t) without chattering in Sliding Mode Control

Another weak point of the Sliding mode control is the relatively slow response time in the first phase of the scheme, also called "reaching phase". In order to reduce the time in which the desired value of the controlled variable is reached, another factor may be introduced that weights the error between the current setpoint and the actual value. If the current error is high, the input variable is adjusted accordingly [3]. In this case, a corresponding factor has not been implemented since the system's response time is sufficient for the intended purpose.

4 Implementation of Model Predictive Control

4.1 Linearization of the System

To control the system via the chosen type of Model Predictive Control, it must be first linearized. For this purpose, two methods have been applied in this work. On the one hand, the angular functions are replaced based on the small angle approximation, that can be used for sufficiently small angles close to the operating point, by the following expressions:

$$sin\alpha(t) \approx \alpha(t) \quad \text{(Valid for sufficiently small angles)}, \tag{14}$$

$$cos\alpha(t) \approx 1 \quad \text{(Valid for sufficiently small angles)}. \tag{15}$$

On the other hand, quadratic parts of the function were linearized. The prerequisite for this is that the system is solely operated in the vicinity of the operating point, in this case the highest position of the pendulum. The more the system states deviate from this operating point, the greater is the error due to the linearization. On basis of the described linearization of the system, the equations of motion (16) and (17) are used hereafter:

$$J\ddot{\alpha}(t) = -F_g l\ \alpha(t) + m_p\ddot{x}(t)\ l\ - k_w\dot{\alpha}(t), \tag{16}$$

$$(m_p + m_{Fgz})\ddot{x}(t) = m_p l\dot{\alpha}(t)\alpha(t) - m_p l\ddot{\alpha}(t) - k_l\dot{x}(t) + F(t). \tag{17}$$

Since the values of the angle α, the angular velocity $\dot{\alpha}$ and thus the angular acceleration $\ddot{\alpha}$ arising from the system using the Sliding Mode Control run against zero, the equation (17) can be simplified to the following function.

$$(m_p + m_{Fgz})\ddot{x}(t) = -k_l\dot{x}(t) + F_{MPC}(t) \tag{18}$$

$F_{MPC}(t)$ constitutes the force that is generated by the Model Predictive Control. Based on the previous considerations, the relevant state-space system is reduced as follows:

$$\begin{bmatrix}\dot{x}(t)\\ \ddot{x}(t)\end{bmatrix} = \begin{bmatrix}0 & 1\\ 0 & \frac{-k_l}{(m_{Fzg}+m_p)}\end{bmatrix}\begin{bmatrix}x(t)\\ \dot{x}(t)\end{bmatrix} + F_{MPC}(t)\begin{bmatrix}0\\ \frac{1}{(m_{Fzg}+m_p)}\end{bmatrix} \tag{19}$$

4.2 Implementation of the control

For the implementation of the MPC the system equations (16) and (18) must be discretized first to obtain an explicit model. For this scheme, the forward Euler method, which is also known as explicit Euler method, can be used. By using this method, the following applies:

$$x(t) = x(k-1), \tag{20}$$

$$\dot{x}(t) = \dot{x}(k-1), \tag{21}$$

$$F_{MPC}(t) = F_{MPC}(k-1), \tag{22}$$

and

$$\dot{x}(t) = \frac{x(k)-x(k-1)}{T_s}, \tag{23}$$

$$\ddot{x}(t) = \frac{\dot{x}(k)-\dot{x}(k-1)}{T_s} \tag{24}$$

with $k = 1, 2, \dots, n$.

Where T_s corresponds to the sampling time for the discretization. Thus, the following system in matrix notation results:

$$\begin{bmatrix}x(k)\\ \dot{x}(k)\end{bmatrix} = \begin{bmatrix}0 & \frac{T_s}{k_l\ T_s}\\ 0 & 1-\frac{k_l\ T_s}{(m_{Fzg}+m_p)}\end{bmatrix}\begin{bmatrix}x(k-1)\\ \dot{x}(k-1)\end{bmatrix} + F_{MPC}(k-1)\begin{bmatrix}0\\ \frac{T_s}{(m_{Fzg}+m_p)}\end{bmatrix} \tag{25}$$

$\hat{X}(k)$ $\quad \underline{A_k}$ $\quad \hat{X}(k-1)$ $\quad \underline{B_k}$

and

$$y(k-1) = \underline{C_k}\ \hat{X}(k-1) \tag{26}$$

respectively

$$\hat{X}(k+1) = \underline{A_k}\hat{X}(k) + \underline{B_k}\ \vec{F}_{MPC}(k) \tag{27}$$

$$y(k) = \begin{bmatrix}1\\ 0\end{bmatrix}\ \hat{X}(k) \tag{28}$$

with $k = 1, 2, \dots, n$

Based on these equations, the state variables for P steps can be predicted. For example, for k + 1:

$$\hat{y}(k+1) = \underline{C_k}\underline{A_k}\ \hat{X}(k) + \underline{C_k}\underline{B_k}\ \vec{F}_{MPC}(k) \tag{29}$$

By the use of recursion, the two-step distant horizon is calculated as shown in (28):

$$\hat{y}(k+2) = \underline{C_k}\underline{A_k^2}\hat{X}(k) + \underline{C_k}\underline{A_k}\underline{B_k}\,\vec{F}_{MPC}(k) + \underline{C_k}\underline{B_k}\vec{F}_{MPC}(k+1) \quad (30)$$

For the controlled variable the following prediction can be applied:

$$\vec{Y}(k) = [\hat{y}(k+1) \quad \hat{y}(k+2) \quad \dots \quad \hat{y}(k+P)]^T \quad (31)$$

$$\vec{Y}(k) = \underline{G}\vec{X}(k) + \underline{H}\vec{F}_{MPC}(k) \quad (32)$$

With the general matrices that apply for G and H:

$$\underline{G} = \begin{bmatrix} C_k A_k \\ C_k A_k^2 \\ \dots \\ C_k A_k{}^P \end{bmatrix} \quad (33)$$

$$\text{and } \underline{H} = \begin{bmatrix} \underline{C_k}\underline{B_k} & 0 & \dots & 0 \\ \underline{C_k}\underline{A_k}\underline{B_k} & \underline{C_k}\underline{B_k} & \dots & 0 \\ \dots & \dots & \dots & \dots \\ \underline{C_k}\underline{A_k^{P-1}}\underline{B_k} & \underline{C_k}\underline{A_k^{P-2}}\underline{B_k} & \dots & \underline{C_k}\underline{B_k} \end{bmatrix} \quad (34)$$

The following matrices result for the described system of the inverse pendulum with a chosen prediction horizon of two steps:

$$\underline{G} = \begin{bmatrix} C_k A_k \\ C_k A_k^2 \end{bmatrix} \text{ and } \underline{H} = \begin{bmatrix} \underline{C_k}\underline{B_k} & 0 \\ \underline{C_k}\underline{A_k}\,\underline{B_k} & \underline{C_k}\underline{B_k} \end{bmatrix} \quad (35)$$

Hereinafter, an input signal is derived so that the deviation between the desired trajectory and the actual signal is minimized. For this purpose, the following cost function is used:

$$J = \frac{1}{2}\left(\vec{Y_r}(k) - \vec{Y}(k)\right)^T \underline{Q}\left(\vec{Y_r}(k) - \vec{Y}(k)\right) + \frac{1}{2}\vec{F}_{MPC}{}^T(k)\,\underline{R}\,\vec{F}_{MPC}(k). \quad (36)$$

Q and R are weighting matrices for the input and the output signal. The solution for the input signal in order to minimize the cost function and thus keeping the error between the desired and actual value as small as possible, is calculated by:

$$\vec{F}_{MPC} = (\underline{H}^T\underline{Q}\underline{H} + \underline{R})^{-1}\,\underline{H}^T\underline{Q}\left(\vec{Y_r} - G\underline{X}(k)\right). \quad (37)$$

The resulting block diagram of the controlled system by SMC and MPC is shown in figure 5.

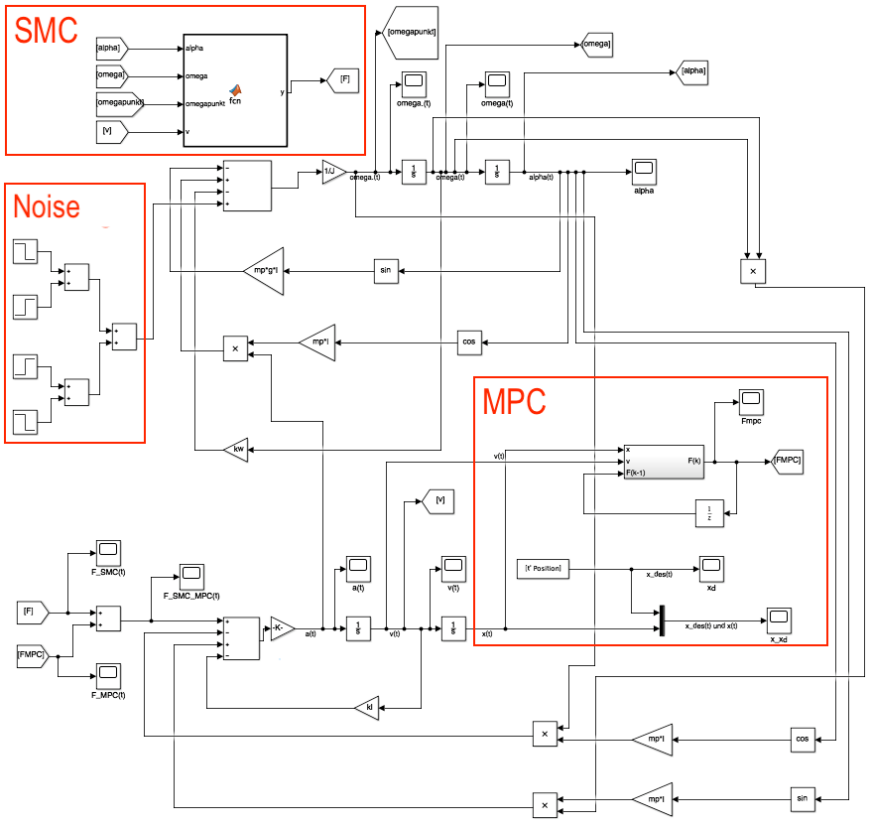

Fig. 5: Block diagram of controlled system by SMC and MPC

5 Behavior of the system

The results after the implementation of the Sliding Mode Control are shown in Fig. 6 and 7. The parameters of the system were chosen as: $m_{Fzg} = 1\,kg,\ m_p = 0{,}1\,kg,\ l = 1\,m,\ g = 9{,}81\frac{m}{s^2},\ J = m_p * l^2,\ k_l = 2\frac{Ns}{rad},\ k_w = 5\frac{Ns}{m},\ \alpha_0 = 0{,}5\,rad,\ \dot{\alpha}_0\ and\ \ddot{\alpha}_0 = 0,\ x, \dot{x}\ and\ \ddot{x} = 0$.

Table 2: assigned values for of equation symbols

Equation-symbol	Meaning	Value	Unit
m_p	Mass pendulum	0,1	kg
M	Mass cart	1	kg
l	Length pendulum	1	m
g	Gravitat. constant	9,81	m/s^2
α	Angle	-0,5	rad
$\dot{\alpha}$	Angular velocity	-	rad/s
$\ddot{\alpha}$	Angular accelerat.	-	rad/s^2
x	Position	-	m
$\dot{x}$	Velocity	-	m/s
$\ddot{x}$	Acceleration	-	m/s^2
k_W	Friction cart	5	Ns/m
k_P	Friction Pendulum	2	Ns/rad
F	Applied force	-	N

In addition, two disturbances were implemented that were directly applied to the angular acceleration $\ddot{\alpha}$. The first disturbance amounts to $10\frac{rad}{s}$ for 0.1 s at 10 s and the second disturbance amounts to $-10\frac{rad}{s}$ for 0.1 s at 20 s.

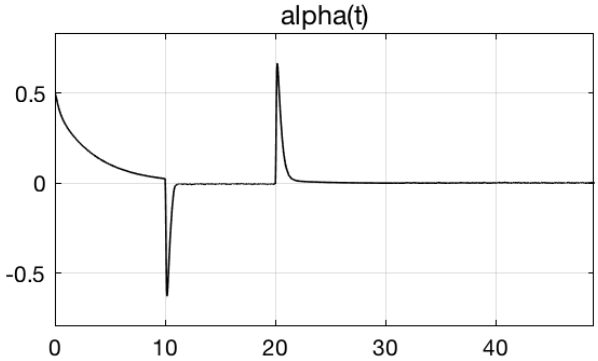

Fig. 6: Angle of the pendulum (Controlled by means of SMC)

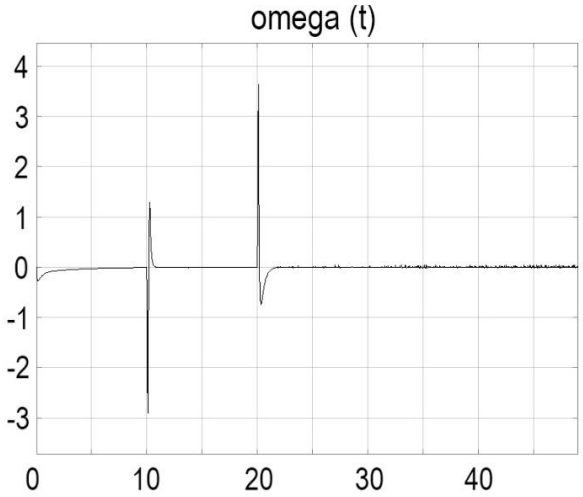

Fig. 7: Angular velocity of the pendulum (Controlled by means of SMC)

The convergence of the state variables angle α and angular velocity $\dot{\alpha}$ can be achieved by using the SMC. Even after the implemented disturbances, the system reaches an angle and an angular velocity close to zero within a short time. This reflects the robustness of the Sliding Mode.

The figures 8 and 9 show how the results change after implementing the Model Predictive Control as the second control system. The parameters of the system were maintained in this case. The sampling time $T_s = 0{,}25\,s$ and the weighting matrices Q and R were added:

$$Q = 1000 * \begin{bmatrix} 1 & 0 \\ 0 & 1 \end{bmatrix} \text{ and } R = \begin{bmatrix} 1 & 0 \\ 0 & 1 \end{bmatrix}. \quad (38)$$

This results in the system behaving as follows:

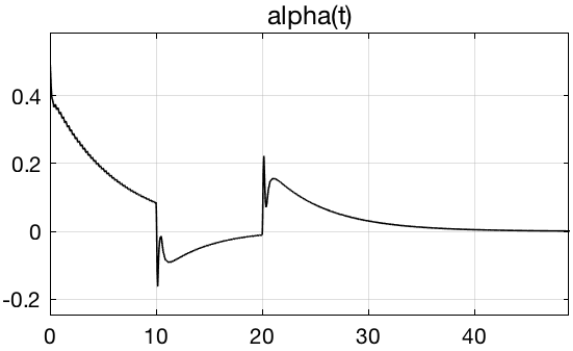

Fig. 8: Angle of the pendulum (SMC and MPC)

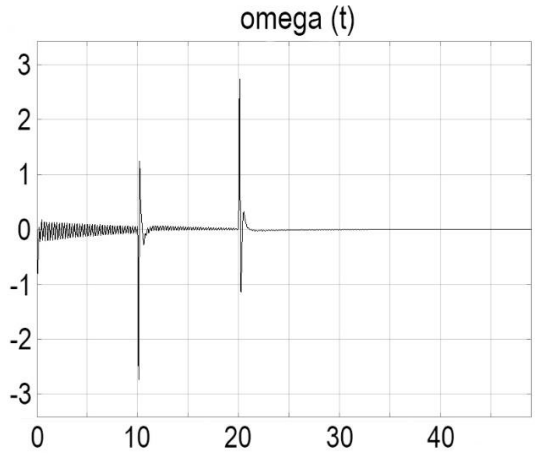

Fig. 9: Angular velocity of the pendulum (SMC and MPC)

From the comparison of the angle of the SMC-controlled system on the one hand and the SMC & MPC-controlled system on the other hand, it can be seen that the rate, at which the angle is regulated, is reduced. This result is obtained because of the differing objectives of the two schemes. Since the cart moves at a certain trajectory, acceleration and speed of the cart are limited. In this case, both forces push the cart in the same direction. In figure 10 the position of the cart is represented.

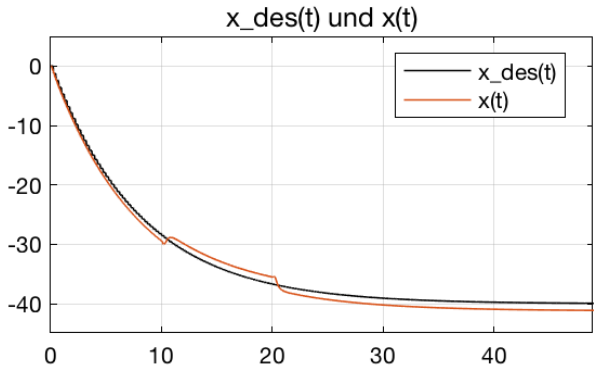

Fig. 10: Comparison of target and actual position

It is noticeable when comparing the desired and actual position, that the actual path of the system exceeds the target value. The system shows the same behaviour without external disturbance. This deviation is a phenomenon that occurs because of the conflict of the two parallel-operated control systems. In addition, the accuracy of the MPC is reduced by the chosen simplifications and the linearization. As a result, there may be a deviation between the desired and the obtained position.

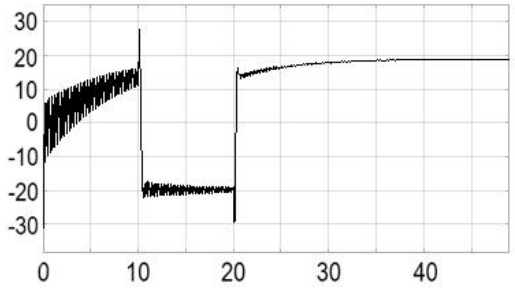

Fig. 11: Force F_{MPC}

As a consequence of the superposition of the input signals and the deviating behaviour of the cart and the pendulum in comparison to the previous, solely SMC-controlled system, the force, that is determined by the Sliding Mode Controller, changes. This force is shown in figure 12.

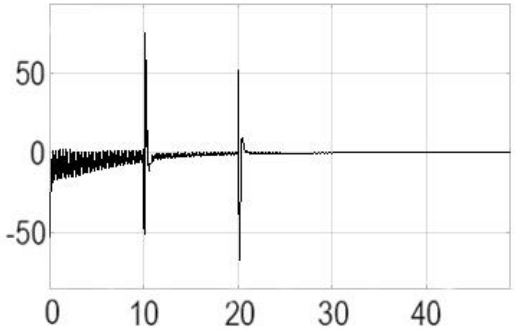

Fig. 12: Force F_{SMC}

It is noticeable that the force switches back and forth with a high frequency because of the conflict of the two input variables despite the implemented saturation function. In this way, both control systems attempt to balance the influence of the respective other control.
Even though the two control systems influence each other, there is a relatively high robustness against external disturbances. Certain deflections of the angle, the angular velocity and position are visible, indeed. However, the speed at which the system is reacting is still relatively high.
In order to further validate the control on the one hand, and to analyse the influence of the superposition of the controls on the other hand, a second simulation was carried out. This time the initial angle was set to -0.5 rad. The corresponding behaviour of the system is shown in figure 13.

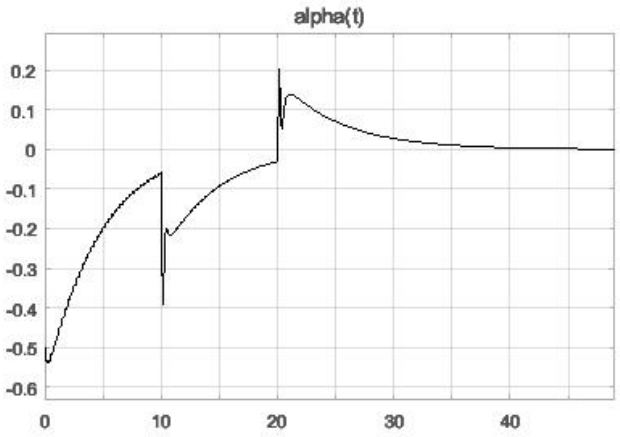

Fig. 13: Angle of the pendulum (SMC and MPC) with a negative initial angle

By analysing this behaviour, it is apparent that the two controls influence each other. It becomes clearly recognizable, e.g., when looking at the time required for the control of the angle compared to the solely SMC-controlled system.

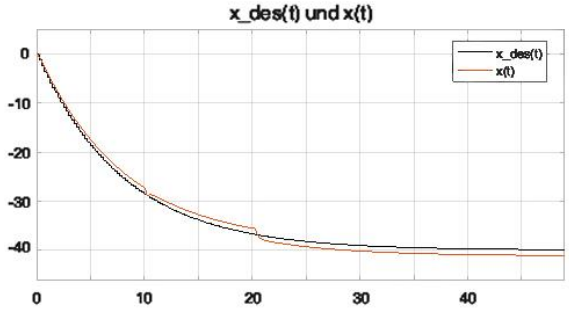

Fig. 14: Target and actual position with a negative initial angle

5 Conclusion and Outlook

The results of this work demonstrate that the use of two different sets of controllers leads to a conflict for the system of the inverse pendulum. For example, a rapid switching of the force as an input signal is necessary in spite of the implemented saturation function.

An expansion and deeper analysis of the impact is possible through the construction of a physical system. For this, a cart with servo motors could be implemented on a rail system. Using such structure, the results could be further validated.

References:

[1] Tröster, F.: Steuerungs- und Regelungstechnik für Ingenieure. 2nd ed., Oldenbourg, München (2005) .

[2] Mahjoub, S., Mnif, F., Derbel, N.: Second-order sliding mode control applied to an inverted pendulum. In: Advances in Robotics, Mechatronics and Circuits, published in 14th International Conference on Sciences and Techniques of Automatic Control & Computer Engineering. IEEE, Sousse (2013).

[3] Mercorelli, P.: Elements of Robotics – Sliding Mode Control. Lecture manuscript summer semester 2018, Leuphana University. Unpublished (2018).

[4] Mercorelli, P.: Elements of Robotics – Control strategies and Model Predictive Control. Lecture manuscript summer semester 2018, Leuphana University. Unpublished (2018).

[5] Honjo, T., Luo, Z., Nagano, A.: Parametric excitation of a biped robot as an inverted pendulum. In: IEEE/RSJ International Conference on Intelligent Robots and Systems. Pp. 3408--3413. IEEE, Nice (2008).

[6] Mercorelli, P.: Elements of Robotics – Dynamics of Robots. Lecture manuscript summer semester 2018, Leuphana University. Unpublished (2018).